

Sources of uniform and 2nd-order gradient fields for testing SQUID performance

Soon-Gul Lee

Korea University, Chungnam, Korea

Received 16 February 2007

SQUID 2차미분기 성능 평가용 균일자기장 및 2차 미분 자기장 발생원

이 순 걸

Abstract

Uniaxial square Helmholtz coils for testing SQUID sensors were designed and their field distributions were calculated. Optimum parameters for maximizing the uniform region in the Helmholtz mode were obtained for different uniformity tolerances. The coil system consists of 2 pairs of identical square loops, a Helmholtz pair for generating uniform fields and the other for the 2nd-order gradient fields in combination with the Helmholtz pair. Full expressions of the axial component of the field were calculated by using Biot-Savart's law. To understand the behavior of the field near the coil center, analytical expressions were obtained up to the 4th-order in the midplane and along the coil axis. The Helmholtz condition for generating uniform fields was calculated to be $d/a=0.544505643$, where $2d$ is the inter-coil distance and $2a$ is the side length of the coil square. Maximized uniform range can be obtained for a given nonuniformity tolerance by choosing d/a slightly lower than the Helmholtz condition. The pure second-order gradient field can be generated by subtracting the Helmholtz field from the field of the 2nd pair with equal magnitudes of the center fields of the two pairs. The coil system is useful for testing balance and sensitivity of SQUID gradiometers.

Keywords : Helmholtz coil, SQUID gradiometer.

I. Introduction

During the course of studying SQUID sensors, one may often encounter lack of proper field sources for

the evaluation of the devices. The purpose of this article is providing bases for designing one's own field sources that are compact but sophisticated enough to meet the precision requirements for SQUID tests.

In our studies on the 2nd-order YBCO SQUID gradiometer [1, 2], sources of uniform fields and the

*Corresponding author. Fax : +82 41 865 0939

e-mail : sglee@korea.ac.kr

2nd-order gradient fields were essential to the characterization of the device. Balancing and gradient sensitivity are the key issues for the evaluation of the 2nd-order SQUID gradiometer. Testing of those properties requires uniform fields and 2nd-order gradient fields. A quick way to generate field distributions is using a current loop. At a position far away from the loop, the field is approximately uniform. One may also use the same coil for testing gradient sensitivity of SQUID gradiometers. However, since such a loop generates fields that contain all orders of gradients, it may be all right for a rough quick test but is not suitable for accurate assessment of SQUID sensors.

Usually, for the purpose of generating uniform fields, a circular-loop Helmholtz-coil system is used. The Helmholtz condition for the circular coils is that the inter-coil distance is equal to the coil radius [3]. In comparison with a circular-loop coil system, a square-loop coil system has relative advantages, such as easier construction and central accessibility. Basic design of a square Helmholtz coil has been reported by Firester [4].

In this work I have analyzed the square-loop coil system theoretically and calculated the optimum parameters to maximize the uniform field zone. Previously, we studied fabrication of a four-square-loop uniaxial Helmholtz coil system and measured field distributions in both Helmholtz and 2nd-order gradient modes [5, 6]. In this paper I report results of more elaborate calculations, especially the parameter conditions for maximized uniform field zone.

II. Square Helmholtz coil

A schematic of the square-loop Helmholtz coil is shown in Fig. 1. In balancing, an axial gradiometer requires a uniform z -component along the z -axis and a transverse gradiometer requires a uniform z -component in the xy plane. By symmetry, only the z -component of the field survives in the xy plane and along the z -axis. Since the 2nd-order gradiometer we are studying is a transverse type, the calculations and

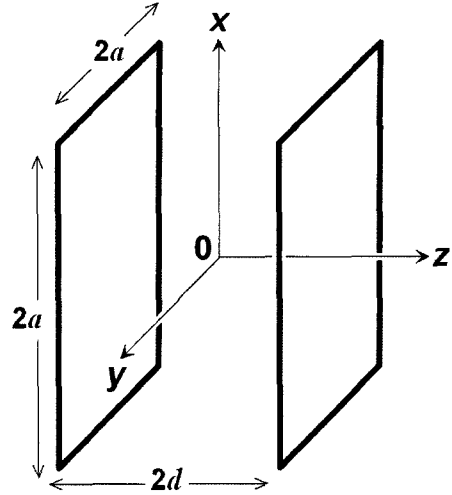


Fig. 1. A schematic of the square-loop Helmholtz coil.

analyses are focused on the z -component of the fields in the xy plane. For axial SQUID gradiometers, I also calculated the z -component along the z -axis. A full analytic expression of the magnetic field is obtained in all space using the Biot-Savart's law.

In Fig. 1, for a one-turn coil pair with current I flowing counterclockwise, the fields in the xy plane and on the z -axis are:

$$B_z(x, y, 0) = \frac{2\mu_0 I}{\pi a} \sum_{i=0}^1 \sum_{j=0}^1 \frac{(-1)^{i+j} a [x + (-1)^i a] [y + (-1)^j a]}{\sqrt{[x + (-1)^i a]^2 + [y + (-1)^j a]^2 + b^2}} \times \left[\frac{1}{[x + (-1)^i a]^2 + b^2} + \frac{1}{[y + (-1)^j a]^2 + b^2} \right] \quad (1)$$

$$B_z(0, 0, z) = \frac{2\mu_0 I}{\pi a} \frac{a^3}{[(z-d)^2 + a^2] \sqrt{(z-d)^2 + 2a^2}} + \frac{a^3}{[(z+d)^2 + a^2] \sqrt{(z+d)^2 + a^2}} \quad (2)$$

Equation (1) is for the xy -plane and (2) for the z -axis. The field was calculated in the xy -plane for different ratios of d to a , denoted by γ ($\equiv d/a$), and plotted in Fig. 2. For $\gamma \geq \gamma_0$ ($\equiv 0.544505643$), field decreases monotonically as the point moves away from the coil center. On the other hand, for $\gamma < \gamma_0$, it has a shallow local minimum at the origin. Field along the z -axis decreases monotonically as z increases.

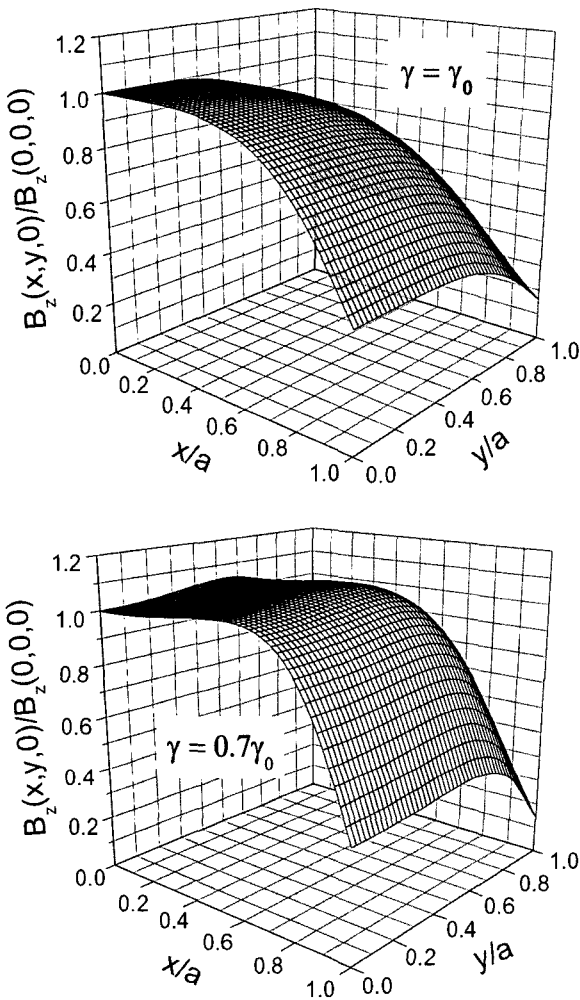


Fig. 2. Surface plots of the field in the xy plane for different ratios of d to a , denoted by γ : (top) $\gamma=\gamma_0$ and (bottom) $\gamma=0.7\gamma_0$. Note that field decreases monotonically as the point moves away from the origin for $\gamma=\gamma_0$ and it has a local minimum at the origin for $\gamma=0.7\gamma_0$.

By Taylor expansion, asymptotic forms of (1) and (2) are obtained as following:

$$\begin{aligned} \frac{B_z(x,0,0)}{B_z(0,0,0)} &= 1 + \frac{1}{2} \frac{5-11\gamma^2-18\gamma^4-6\gamma^6}{(1+\gamma^2)^2(2+\gamma^2)^2} \left(\frac{x}{a}\right)^2 \\ &+ \frac{191-694\gamma^2-138\gamma^4-660\gamma^6+165\gamma^8+210\gamma^{10}+45\gamma^{12}}{8(1+\gamma^2)^4(2+\gamma^2)^4} \left(\frac{x}{a}\right)^4 \\ &+\dots, \end{aligned} \tag{3}$$

$$\begin{aligned} \frac{B_z(0,0,z)}{B_z(0,0,0)} &= 1 - \gamma^2 \frac{5-11\gamma^2-18\gamma^4-6\gamma^6}{(1+\gamma^2)^2(2+\gamma^2)^2} \left(\frac{z}{d}\right)^2 \\ &+ \frac{\gamma^4}{2} \frac{43-352\gamma^2-678\gamma^4-280\gamma^6+145\gamma^8+140\gamma^{10}+30\gamma^{12}}{(1+\gamma^2)^4(2+\gamma^2)^4} \left(\frac{z}{d}\right)^4 \\ &+\dots \end{aligned} \tag{4}$$

where,

$$B_z(0,0,0) = \frac{2\mu_0 NI}{\pi a} \frac{2}{(1+\gamma^2)\sqrt{2+\gamma^2}}. \tag{5}$$

In (3) and (4), the second-order terms vanishes for $\gamma=\gamma_0\approx 0.544505643$, which is the Helmholtz condition. Helmholtz fields are reduced to:

$$\frac{B_z(x,0,0)}{B_z(0,0,0)} = 1 - 0.40017 \left(\frac{x}{a}\right)^4 + \dots, \tag{6}$$

$$\frac{B_z(0,0,z)}{B_z(0,0,0)} = 1 - 0.07072 \left(\frac{z}{d}\right)^4 + \dots. \tag{7}$$

The fields along the x -axis and the z -axis are plotted in Fig. 3. In the figure, both fields near the center are biquadratic as expected in (6) and (7). The biquadratic dependence persists in a quite large extent up to $x/a\sim 0.4$ and $z/d\sim 0.4$. For a nonuniformity tolerance of 10^{-4} , the uniform region is $x/a < 0.125$ for

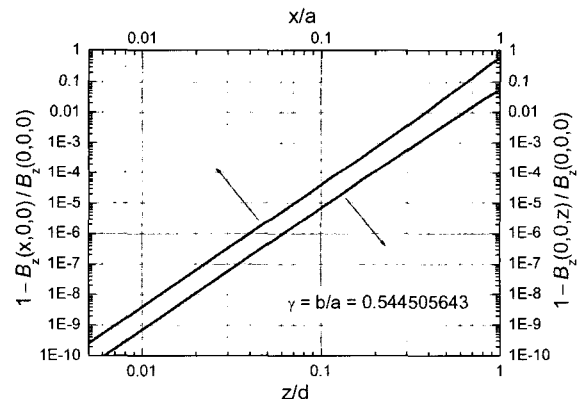


Fig. 3. Field distributions of the Helmholtz coil at $\gamma=\gamma_0$ along the x -axis and the z -axis. Note that the fields are biquadratic near the center.

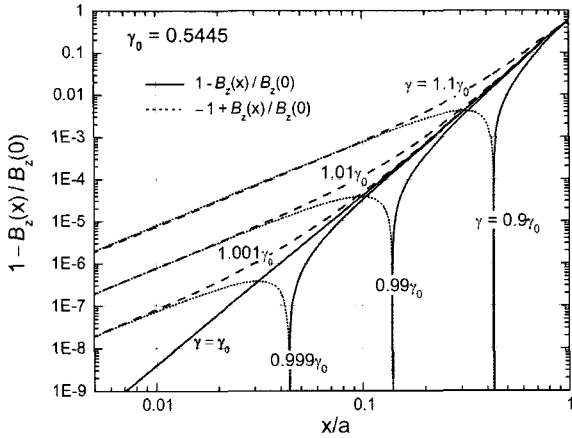


Fig. 4. Field distributions along the x -axis for different values of γ . Field changes monotonically for $\gamma \geq \gamma_0$ and changes sign for $\gamma < \gamma_0$ due to the local minimum at the center.

the transverse field and $z/d < 0.194$ for the axial field. The uniform region for the transverse field can be further expanded by choosing γ less than 1, depending on the nonuniformity tolerance.

Fig. 4 shows distributions of the transverse field for different values of γ . For $\gamma > 1$, the field distribution becomes quadratic near the coil center and the nonuniformity increases with increasing γ . On the other hand, for $\gamma < 1$, the field distribution function has a shallow minimum at the center as shown in Fig. 2 (b). In Fig. 4, the relative field changes sign from - to + inside the position where the field has the same magnitude as that of the coil center and becomes quadratic with larger magnitudes compared with the Helmholtz field. For a given nonuniformity tolerance, one can get a uniformity range wider than that of the Helmholtz case.

Fig. 5 shows the distributions of off-the-Helmholtz-fields for 3 different values of nonuniformity tolerance, 10^{-4} , 10^{-3} , and 10^{-2} . For the tolerance of 10^{-4} , the largest uniformity range, $|x/a| < 0.193$, can be obtained at $\gamma = 0.984\gamma_0$. This range is 54 % larger than the Helmholtz range of $|x/a| < 0.125$. For the other two tolerances, optimum values of γ and the uniformity range $\delta (=x/a)$ are shown in Table 1 in comparison with the Helmholtz values. In any case, a larger uniformity range is

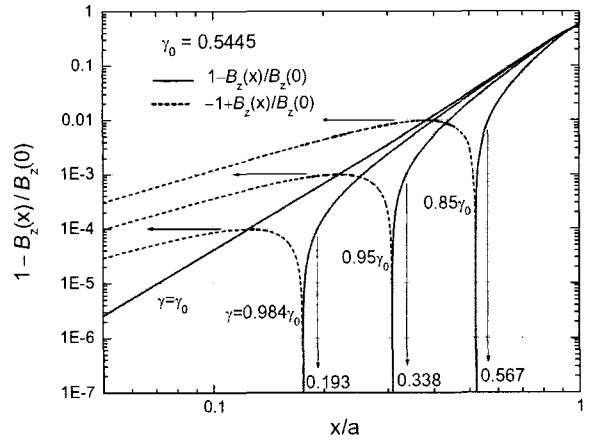


Fig. 5. Field distributions for 3 different values of γ , 0.984, 0.95, and 0.85, at which the uniform range is maximum for nonuniformity tolerances (ζ), 10^{-4} , 10^{-3} , and 10^{-2} .

Table 1. Uniformity ranges for 3 values of uniformity tolerances. $\delta = x/a$.

Tolerance	Optimum γ	Uniformity range $\delta(\gamma)$	$\delta(\gamma_0)$	$\delta(\gamma)/\delta(\gamma_0)$
10^{-4}	0.984	0.193	0.125	1.54
10^{-3}	0.95	0.338	0.221	1.53
10^{-2}	0.85	0.567	0.385	1.47

guaranteed. These results are useful for those who want to prepare uniform field sources in a limited experimental space. Less use of materials, easier construction, and easier central access are additional advantages.

Axial fields are monotonic for all values of γ and the deviation becomes larger as γ increases. The Helmholtz field has the largest uniformity region.

III. Second-order gradient coil

Equations (3) and (4), and Fig. 4 show that coil pairs with off-the-Helmholtz-condition ($\gamma \neq \gamma_0$) have a nonzero quadratic term. Combining these coils with the Helmholtz pair can generate pure second-order gradient fields. Fig. 6 shows a schematic of a four-

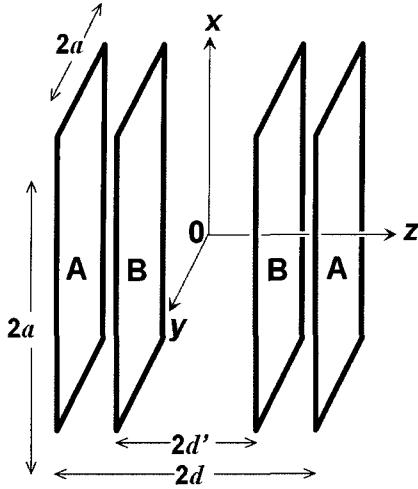


Fig. 6. A schematic of the four-identical-square-loop coil system for generating the second-order gradient fields.

square-loop coil system generating the pure second-order field gradients. AA is a Helmholtz coil pair of N_A turns and BB is an off-the-Helmholtz-condition pair of N_B turns. If current I flows in opposite directions in those two pairs and the number of turns N_A and N_B are chosen so that the central fields cancel each other, the first nonzero term is quadratic and thus the system becomes a source of the second-order gradient fields. The system becomes a uniform field source by running the current only in the Helmholtz pair AA. The four-loop coil system can be used for both balancing test and gradient sensitivity measurement of second-order SQUID gradiometers.

Fig. 7 shows the results of calculation for both transverse and axial fields with $N_A/N_B = 1.2$, $\gamma_A = \gamma_0 = 0.5445$ and $\gamma_B = 0.3515$. In both cases, the fields are quadratic dependence on the position up to x/a , $z/d \cong 0.35$. Outside the quadratic region, while the axial field increases monotonically, the transverse field reaches a maximum at around $x/a = 0.75$ and then decreases abruptly. Except near the coil edges, the fields are calculated as following:

$$\frac{B_z(x,0,0)}{2\mu_0 N_B I / \pi a} = 0.3600 \left(\frac{x}{a} \right)^2 + \dots, \quad (8)$$

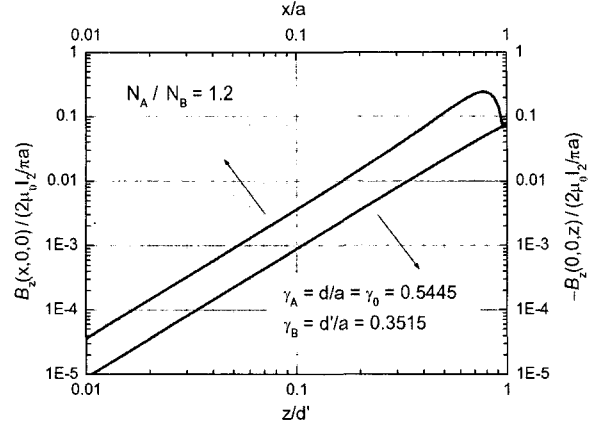


Fig. 7. Field distributions of the 2nd-order gradient mode for $N_A/N_B = 1.2$ at the optimized condition, $\gamma_A = \gamma_0 = 0.5445$, and $\gamma_B = 0.3515$.

$$\frac{B_z(0,0,z)}{2\mu_0 N_B I / \pi a} = -0.08804 \left(\frac{z}{d} \right)^2 + \dots, \quad (9)$$

Results of experiments based on these calculations well agreed with theory and have been reported in [5], [6].

IV. Summary

A uniaxial four-identical-square-loop coil system was designed for evaluating SQUID properties and the field distributions have been calculated by using Biot-Savart's law. The system consists of 2 pairs of identical square loops, one for producing Helmholtz fields and the other for 2nd-order gradient fields in combination with the Helmholtz pair. The Helmholtz condition was calculated to be $d/a = 0.544505643$. Maximized uniform range for a given nonuniformity tolerance was obtained by choosing d/a slightly lower than the Helmholtz condition. Expression of the pure second-order gradient field was obtained by subtracting the Helmholtz field from the field of the off-the-Helmholtz 2nd pair with equal magnitudes of the center fields of the two pairs. The coil system is useful for testing balance and sensitivity of SQUID gradiometers.

Acknowledgments

This work was financially supported by the Ministry of Commerce, Industry and Energy, Republic of Korea.

References

- [1] S. G. Lee, S. M. Park, C. S. Kang, K. K. Yu, I. S. Kim, and Y. K. Park, "Fabrication and magnetocardiography application of the second-order superconducting quantum interference device gradiometer made from a single-layer of $\text{YBa}_2\text{Cu}_3\text{O}_7$ film," *Appl. Phys. Lett.*, 84(4), 568-570 (2004).
- [2] S. G. Lee, S. M. Park, C. S. Kang, I. S. Kim, "Magnetocardiographic performance of single-layer second-order YBCO SQUID gradiometers," *IEEE Trans. Appl. Supercond.*, 15(2), 801-804 (2005).
- [3] See, for example, J. R. Reitz and F. J. Milford, *Foundations of Electromagnetic Theory*, 2nd ed., New York, Addison Wesley, 1967, pp. 156-157.
- [4] A. H. Firester, "Design of square Helmholtz coil system," *Rev. Sci. Instrum.* 37(9), 1264-1265 (1966).
- [5] S. G. Lee, C. S. Kang, and J. W. Chang, "A square-loop Helmholtz coil system for the evaluation of a single-layer 2nd-order high- T_c SQUID gradiometer," to be published in *Physica C*.
- [6] S. G. Lee, C. S. Kang, and J. W. Chang, "Square loop coil system for balancing and calibration of second-order SQUID gradiometers," to be published in *IEEE Trans. Appl. Supercond.*